Soil protists can actively redistribute beneficial bacteria along *Medicago truncatula* roots

Christopher J. Hawxhurst[Δa], Jamie L. Micciulla[Δb], Charles M. Bridges[b], Leslie M. Shor[a,c], Daniel J. Gage[b#]

[Δ]Co-first Authors

[a]Department of Chemical & Biomolecular Engineering, University of Connecticut, Storrs, CT, USA

[b]Department of Molecular and Cellular Biology, University of Connecticut, Storrs, CT, USA

[c]Center for Environmental Sciences & Engineering, University of Connecticut, Storrs, CT, USA

#Address correspondence to Daniel Gage, Daniel.Gage@UConn.edu

Christopher J. Hawxhurst and Jamie L. Micciulla contributed equally to this work. Author order was determined alphabetically.

Keywords: Protist, Soil, Plant Beneficial Bacteria, Transport

Abstract

The rhizosphere is the region of soil directly influenced by plant roots. The microbial community in the rhizosphere includes fungi, protists, and bacteria, all of which play a significant role in plant health. The beneficial bacterium Sinorhizobium meliloti infects growing root hairs on nitrogen starved leguminous plants. Infection leads to the formation of a root nodule, where S. meliloti converts atmospheric nitrogen to ammonia, the usable form of nitrogen for plants. However, S. meliloti, often found in biofilms, travels slowly; whereas infectible root hairs are found at the growing root tip, potentially causing many root hairs to remain uninfected by S. meliloti when it is delivered as a seed inoculant. Soil protists are an important component of the rhizosphere system who prey on soil bacteria and have been known to egest undigested phagosomes. We show that the soil protist, Colpoda sp., plays an important role in transporting S. meliloti down Medicago truncatula roots. By using pseudo-3D soil microcosms we directly observed the presence of fluorescently labelled S. meliloti along M. truncatula roots and track the displacement of bacteria over time. In the presence of Colpoda sp., S. meliloti was detected 44 mm, on average, farther down the roots, compared with the Bacteria Only Treatment. Facilitating bacterial transport may be an important mechanism whereby soil protists promote plant health. Protist facilitated transport as a sustainable agriculture biotechnology has the potential to boost efficacy of bacterial inoculants, avoid overuse of nitrogen fertilizers, and enhance performance of no-till farming practices.

Importance

Soil protists are an important part of the microbial community in the rhizosphere. Plants grown with protists fare better than plants grown without protists. Mechanisms through which protists support plant health include nutrient cycling, alteration of the bacterial community through

selective feeding and consumption of plant pathogens. Here we provide data in support of an additional mechanism: protists act as a transport vectors for bacteria. We show that protist-facilitated transport can deliver plant-beneficial bacteria to the growing tips of roots that may otherwise be sparsely inhabited with bacteria from a seed-associated inoculum. By co-inoculating *Medicago truncatula* roots with both *Sinorhizobium meliloti*, a nitrogen fixing legume symbiont, and the ciliated protist, *Colpoda sp*., we show bacteria are distributed an average of 44 mm farther down plant roots than when the plants are inoculated by bacteria alone. Co-inoculation with shelf-stable encysted soil protists may be employed as a sustainable agriculture biotechnology to better distribute beneficial bacteria and enhance the performance of inoculants.

Introduction. The rhizosphere is the zone of soil surrounding plant roots that is under the influence of the root. This soil fraction contains 5 to 100 times more organisms per unit volume than adjacent bulk soil (1). Up to 40% of carbon assimilated by plants is contributed back to the soil as rhizo-deposits (2). In return for these carbon-rich root exudates, plants often benefit from microbial activity through a variety of mechanisms such as moisture retention, pathogen suppression, plant-hormone synthesis and the release of recalcitrant nutrients (3, 4). Furthermore, some soil dwelling bacteria, such as those from the family Rhizobiaceae, beneficially infect leguminous roots and directly provide fixed nitrogen in exchange for TCA cycle intermediates.

The functioning of soil and rhizosphere systems emerges, in part, from biological communities interacting in a spatially structured environment (5–11). In trying to better understand the importance of biological factors on the properties of soil, research has been dedicated to the study and interaction of different bacterial species and plants in spatially-constrained systems (6, 9, 10). Protists form an additional, important, and sometimes overlooked component of the soil system. The presence of protists in addition to bacteria can promote and enhance size and weight of plant roots and shoots over bacteria alone (12). Protist-associated enhancement to plant health can arise through several different mechanisms. In the "microbial loop" hypothesis, protists recycle limiting nutrients by grazing on the microbes fed by root exudates (13–17). Protists may also alter the microbial composition of the rhizosphere through selective grazing (17, 18). A third potential mechanism is that protists may improve plant health by acting as a transport vector: moving bacteria or other "cargo" along downward-growing roots (19–21). Similar examples include transport of fungal spores hitchhiking on bacterial flagella (37). Other examples are given in recent reviews (38, 39).

75 Plant growth promoting rhizobacteria (PGPR) are beneficial soil bacteria used in
76 agriculture to improve yields and disease resistance. PGPR-mediated nutritional effects include
77 symbiotic nitrogen fixation, non-symbiotic nitrogen fixation, release of recalcitrant nitrogen from
78 soils, phosphate solubilization, and iron delivery (2–5). Commercially-used PGPR include many
79 species of nitrogen-fixing bacteria: *Azospirillum* spp., *Azotobacter* spp., *Pseudomonas* spp.,
80 *Bacillus subtilis* strains, *Bacillus megaterium* strains and *Trichoderma* spp. (a fungal genus) (2).
81 Many additional species are under investigation in laboratory, greenhouse, and field trials, but
82 have not yet been commercialized.

83 PGPR are typically inoculated onto seeds before planting or they are directly applied to the
84 soil during planting. Soil bacteria usually grow as biofilms and spread very slowly. Thus, bacteria
85 inoculated onto, or near, seeds often do not leave the area of inoculation and do not establish a
86 population on the root large enough to provide beneficial services (6–9, 22). Further, symbiotic
87 infection of root hairs with nitrogen-fixing rhizobia, such as *Sinorhizobium meliloti*, often occurs
88 at growing root hairs which are located growing at growing root tips. Since roots grow at their tips,
89 these are actively moving away from the soil surface where the seed was planted. The relative lack
90 of bacteria at the root tip can cause a decreased rate of symbiotic infection and nodulation (23).

91 Soil protists have the potential to act as transport vehicles for bacteria. Soybeans roots can
92 grow at ~3000 μm per hour (24). For comparison, the spreading rate of biocontrol *P. fluorescens*
93 biofilms is less than 10 μm per hour (25), while ciliated protists can swim at speeds up to 400 μm
94 per second for short periods (26). We have shown in vitro that protists can transport beads and
95 bacteria much faster than they could travel without protists (19). In situ, protists are known to carry
96 bacteria, most commonly as intracellular parasites, for example when *Legionella* spp. infect
97 aquatic amoeba or *Campylobacter* spp infect ciliates [28, 40]. Also, bacterial transport by protists

98 has been demonstrated in the soil amoeba *Dictyostelium discoideum*, which can carry bacteria to
99 new habitats (26, 27). Although protists graze on bacteria, ingestion is not always fatal (28).
100 Further, bacteria have been observed attached to the outer surfaces of protists, thus providing a
101 means for transport that does not require ingestion (19). We propose protists contribute to the
102 rhizosphere community, in part, through their capacity to spatially redistribute bacteria. The goal
103 of this study was to test the hypothesis that a protist species, despite grazing, could enhance
104 bacterial dispersal along root systems. We measured the spatial distribution of fluorescently
105 labelled *S. meliloti* through soil-containing mesocosms over time in the presence and absence of a
106 soil-isolated, ciliated, protist from the genus *Colpoda*.

107 **Experimental Materials and Methods**

108 **Model soil.** Sterile model soil was comprised of play sand (Quikrete) and fine vermiculite
109 combined 1:1 in a soil mixer. The mix was fractionated by sieving and the 125-250 µm fraction
110 and 63–125 µm fraction were combined 1:2 to emulate the particle sized distribution of a model
111 sandy loam (11).

112 **Plants.** *Medicago truncatula* is a model legume that offers uniform growth and natural symbiosis
113 with *S. meliloti.* To synchronize the plants, we sterilized the seeds by successive washing with
114 95% ethanol for 30 min, 10% bleach for 15 min, and sterile diH_2O for 15 min on a shaking platform
115 at 80 rpm. Next, we imbibed seeds in sterile diH_2O in the dark for 24 h. Then, we rinsed the seeds
116 in sterile diH_2O, transferred them to a sterile plastic petri dish, and stored them in an inverted dish
117 in darkness overnight for germination.

118 **Bacterial strain construction.** The BioFAB plasmid pFAB2298 was kindly provided by Vivek
119 Mutalik (29). We amplified the expression cassette containing Ptrc-BCD2-mRFP1 with Phusion
120 polymerase (Fisher) as a single unit from pFAB2298 using primers 5'-

121 ATCTGCAGGCTTCCCAACCTTACCAG-3' and 5'-
122 CAGTATCGATAGTCAGTGAGCGAGGAAGC-3', which contain 5' *Pst*I and *Cla*I restriction
123 sites, respectively. We digested the resulting 1.244 kb amplicon with *Pst*I and *Cla*I (New England
124 Biolabs) and cloned it into pBlueScript II SK(+) to create pCMB21. We digested the expression
125 cassette from pCMB21 using AvrII and EcoRI-HF (New England Biolabs) and cloned into
126 pSEVA551 (*tetA*, RSF1010 *oriV*) to create pCMB35 (30). We introduced plasmid pCMB35 into
127 *S. meliloti* strain Rm1021 by electroporation in a 1 mm gapped cuvette at 2200 V and plated on
128 TY medium (6 g/L tryptone (BD), 3 g/L yeast extract (BD), 0.38 g/L $CaCl_2$ (Acros), 15 g/L agar
129 (BD)), amended with 500 µg/mL streptomycin sulfate (Acros) and 5 µg/mL tetracycline
130 hydrochloride (Sigma).
131 **µ-Rhizoslide construction.** We constructed small-scale, soil-containing, mesocosms from the
132 rhizoslide designed by Le Marié, *et al* (31). Mesocosms were comprised of a 3D printed spacer
133 with a hollow opening which was filled with model soil. This was sandwiched between two 50 ×
134 75 mm glass slides. We refer to our version as a "µ-rhizoslide". After several design iterations to
135 balance space for root growth, plant health, and imaging consistency, the final spacer design
136 features a 1.5 cm wide, 7.5 cm long main channel with a 1.5 mm connector at the top of the channel
137 to stiffen the spacer and limit deformation (Fig. 1).
138 Our µ-rhizoslides allow for direct optical imaging of the growing plant root and minimize
139 any water-based transport effects. The µ-rhizoslide assembly (Fig 1A) consists of a 3D printed
140 spacer sandwiched between two 50 × 75 mm glass slides, with a 50 × 85 mm filter paper wick
141 added between the back of the 3D printed spacer and the rear microscope slide, to allow for plant
142 hydration without gravity driven, bulk, water flow. Spacers were designed using Solidworks 2018,
143 imported into PreForm software and printed on a Formlabs Form 2 stereolithography 3D printer

144 using Clear Resin GPCL04 (Formlabs, Somerville, MA). To improve biocompatibility, printed
145 spacers were treated to leach labile resin or crosslinker using a protocol adapted from Kadilak et
146 al. (32). Treatment is necessary because un-crosslinked monomer can have antimicrobial
147 properties (33). Briefly, we soaked 3D printed spacers in an isopropanol bath for 30 min, then
148 rinsed with additional isopropanol from a squeeze bottle. This treatment was repeated twice more
149 to ensure there was no remaining un-crosslinked resin.

150 Assembly of μ-rhizoslides proceeded as follows. The 3D printed spacer resting on a glass
151 slide was filled with sterile diH_2O-saturated sterile model soil, then covered with a filter paper
152 wick, and closed by affixing another glass slide on the front of the μ-rhizoslide assembly.
153 Germinated seeds were placed in a small depression at the top of the soil column. We kept the μ-
154 rhizoslides separated by treatment in transparent plastic boxes with each μ-rhizoslide positioned
155 45° off vertical with the filter paper wick on the top face to encourage root growth directly against
156 the glass slide on the bottom of the assembly. This arrangement also helped protect the roots from
157 light exposure, as we kept the μ-rhizoslide boxes in a growth chamber under a 16:8 h light:dark
158 cycle at 23 °C to maintain the plants. We allowed the plants to grow in the μ-rhizoslides for 2 d to
159 insure root establishment prior to inoculation and imaging.

160 **Growth of protists and bacteria.** The protists used in this experiment were identified by 18s
161 rRNA sequencing as a belonging to ciliate genus *Colpoda*, which we refer to as UC1 (34). UC1
162 was isolated from a bean rhizosphere and cultured in the lab in Page's Saline Solution (35). UC1
163 was maintained in 25 cm3 tissue-culture flasks (Thermo Scientific #130192) with 5 mL of Page's
164 Saline to allow for full oxygenation for optimal protist growth. Protists were fed heat-killed *E. coli*
165 DH5a, inoculated at OD595 = 0.005 as measured in 100 μL of a suspension in a 96-well microtiter
166 dish. Prior to plant inoculation, UC1 cultures were stored in darkness, at room temperature, for 3

167 weeks. Cysts were removed from the cell culture flask using a sterile cell scraper, washed twice
168 with Page's Saline Solution, then resuspended in 100 µL of the same medium. Protist cysts were
169 washed, concentrated, and counted the day of inoculation. We estimated the concentration of the
170 cysts by averaging the number of cysts counted in three 1 µL spots under a microscope. For
171 experiments using trophozoites (protists in their active growing stage) encysted protist cultures
172 were washed two days before inoculation to allow for excystment. Once most protists had emerged
173 from the cysts and were active they were concentrated, counted, and inoculated them onto plants
174 that had been previously established in µ-rhizoslides, as outlined above.

175 Bacteria inoculants were prepared as follows. A single colony of *S. meliloti* strain
176 Rm1021/pCMB35 was picked from a TY + tetracycline (5 µg/ml) plate, grown in a 125 ml flask
177 containing 25 ml of liquid TY + tetracycline (5 µg/ml) at 30 °C with shaking at 160 rpm for 3 d.
178 Cells were washed twice with Page's saline solution then resuspended in Page's to OD_{595} = 0.1.
179 OD_{595} was determined in a 96-well microtiter dish using 100 µL of cell suspension.

180 **Experimental design.** We prepared 10 µL inocula for five replicate µ-rhizoslides for each of the
181 following three treatments: 1) Page's medium alone (Control); 2) 10^7 CFU Rm1021/pCMB35
182 in Page's medium (Bacteria Only); 3) 10^7 CFU Rm1021/pCMB35 + 1.5×10^3 *Colpoda* UC1 in
183 Page's medium (Bacteria + Protist). To prevent a large fluorescent bloom at the inoculation site,
184 we delivered inocula directly onto the root/shoot interface with the µ-rhizoslide positioned wick-
185 side down, opposite of the orientation used for growth (described above), to avoid gravity-driven
186 flow of the inoculum along the front glass slide. Inoculated µ-rhizoslides were stored wick-side
187 down for one (1) hour post inoculation, then returned to their normal orientation so roots were
188 facing down for the remainder of the experiment. µ-rhizoslides were grouped by treatment and

189 positioned in the growth chamber as described above. Every 4th day, μ-rhizoslides were alternately
190 watered with either sterile diH_2O or a modified Hoagland's solution (19).

191 **Imaging and Image Analysis.** Once per week, we imaged the entire soil area of each μ-rhizoslide
192 using tiled brightfield and fluorescent images using a Zeiss AXIO-Observer Z1 inverted
193 microscope (Carl Zeiss Inc., Germany) with an AxioCam MRm Rev.3 camera (1348 × 1040 pixels,
194 6.45 × 6.45 μm/pixel). We used a 5× Zeiss EC Plan-Neofluar 5×/0.16 M27 lens and set the camera
195 to collect 585-binned photos (2 × 2 binning). The transmission-based brightfield light equipped on
196 the microscope could not illuminate through the 0.5 cm of soil, so we moved the brightfield lamp
197 to an external stand and focused it on the soil surface at the front of the μ-rhizoslide. For fluorescent
198 imaging, we found 570 nm excitation and 620 nm emission filters gave the strongest fluorescent
199 signal for *S. meliloti* Rm1021/pCMB35. We used the Zeiss Zen Pro 2.3 software to stitch a single
200 207-megapixel image (29341 × 7072 pixels) from each set of 585 photos. We then exported each
201 image as 12-bit grayscale TIFF at full resolution.

202 For image analysis, the stitched fluorescent images were imported into MATLAB and
203 converted into 29341 × 7072 matrices. Since we took steps to limit bacterial fluorescent
204 bloom on images taken the same day as the inoculation (Week 0), we were able to use the
205 fluorescent images from week 0 as a measure of background fluorescence from sources like the
206 3D printed spacer, and mica particles in the soil. We subtracted the Week 0 tiled fluorescent image
207 of each μ-rhizoslide from the tiled fluorescent images of all subsequent weeks to remove the
208 aforementioned background fluorescence. Any subsequent negative pixel value was set to 0. In
209 addition, tiled images were cropped to remove the non-soil portion, eliminating fluorescence from
210 the 3D printed spacers. As *S. meliloti* bacteria was predominately found towards the center of the

211 soil channel, along the roots, removing the background from the 3D spacer this way had a minimal
212 effect on the bacterial fluorescence signal.

213 We partitioned the photo matrixes into sections approximately 1 mm in length along the
214 root axis (386 × 7072 pixels), encompassing the full width of the soil region. Next, we determined
215 the fraction of the area of each section with a non-zero fluorescence signal. We define "normalized
216 fluorescent area" as the number of nonzero pixels divided by the total number of pixels in the
217 section. We then plotted the normalized fluorescent area versus distance of the section from the
218 soil-air interface (Fig 3). We define "furthest displacement" as the 1-mm partition with at least
219 10% normalized fluorescent area. We then plotted the mean furthest vertical and horizontal
220 displacement values of the five replicates for each treatment versus distance from the soil-air
221 interface with their standard deviation (Fig 4 & Fig 5). We used one-way ANOVA using the values
222 for furthest progress of the fluorescent signal for each treatment to determine the statistical
223 significance of the different treatments.

224 We created composite images for ease of visualization of the progress of the fluorescent
225 signal (Fig 2). We used the Week 3 brightfield images for each rhizoslide trial, and overlayed these
226 images with weekly greyscale fluorescent images colored coordinated to the week. These
227 composite images were not used for quantitative data analysis.

228 **Post-imaging quantification of *Colpoda sp.* and *S. meliloti* in u-rhizoslides.** After the final
229 imaging, μ-rhizoslides were disassembled and roots were separated from the bulk soil. Roots were
230 cut into "upper" and "lower" halves beginning 2.5 cm from the root/shoot interface. Root weight
231 was recorded, then the root sections were suspended in 10 times their weight in Page's medium in
232 50 ml conical tubes. Roots were vortexed for 1 minute at medium speed on a tabletop vortex mixer.

233 For bacteria abundance, 10-fold dilutions were made in Page's medium and 10 µL spots
234 were placed onto TY + tetracycline (5 µg/ml) agar plates and incubated at 30 °C for 3 days.
235 Colonies were counted, and the total number of *S. meliloti* strain Rm1021/pCMB35 was estimated
236 for each root section.

237 To estimate protist abundance, 3-fold dilutions were carried out in a 96 well microtiter dish
238 using Page's medium+ heat-killed *E. coli* DH5a (OD_{595} = 0.05). Eight replicate dilutions were
239 done for each root section. Microtiter dishes were incubated at room temperature in darkness for
240 1 week. Presence of protists in each well was recorded and assumed that "at least one" protist made
241 it into wells that contained protists. The Minimum Recovered Number per ml (MRN/ml) of protists
242 was back calculated as follows:

243 $MRN/ml = 10 * 3^{(\text{farthest positive dilution factor} - 1)}$

244

245 **Results**

246 **µ-rhizoslides allow convenient, long-term tracking of plant root development.** µ-rhizoslides
247 were constructed as a smaller version of the rhizoslides designed by C. L. Marie (31), and
248 optimized for microscopy and increased through-put. Root growth and behavior is easily
249 monitored on a standard inverted microscopy with the smaller µ-rhizoslides. Plant roots occupy a
250 region 15 × 75 mm and can be readily imaged as a series of overlapping tiled images (Fig 2). When
251 not being imaged the µ-rhizoslides were kept at a 45-degree angle to promote root growth directly
252 against the glass slide. This successfully facilitated direct microscopy of the roots without
253 removing the surrounding soil. Brightfield microscopy was used to image root tissue of which
254 allowed monitoring of primary, secondary and tertiary roots. Images were collected once a week

255 for 4 weeks after planting. This demonstrated the ability of the μ-rhizoslide to support plant growth
256 for extended periods: a typical requirement of many root-growth experiments.
257 **Distribution of *S. meliloti* on plant roots increases in the presence of protists.** Inoculation of
258 seeds with beneficial bacteria, while effective under some circumstances, often fails to provide
259 maximum benefits to the grown plant because the bacteria are not effectively distributed along the
260 growing root system. Soil protists, which often prey on bacteria, may enhance bacterial movement
261 by physically moving them as a result of the feeding process, or by excreting still living bacteria
262 after they have been ingested. In order to test this hypothesis, the nitrogen fixing symbiont
263 *Sinorhizobium meliloti* strain Rm1021 was transformed with plasmid pCMB35 which directs the
264 constitutive expression of mRFP. The movement and growth of Rm1021/pCMB35 was tracked
265 by fluorescent microscopy in the μ-rhizoslides over the course of four weeks under three
266 conditions: Control (plant only); Bacteria (plant + Rm1021/pCMB35 only) and Bacteria + Protist
267 (plant + protist and Rm1021/pCMB35) (Fig 4). When comparing the progress of the fluorescent
268 signal, indicative of Rm1021/pCMB35, a significant difference between treatments was
269 demonstrated by ANOVA for all time points after Week 0 ($p < 0.005$). Rm1021/pCMB35 in the
270 Bacteria + Protist Treatment colonized an average of 44 mm more root when compared with the
271 other treatments by Week 2. Data from later time points showed increased variation in the
272 movement of Rm1021/pCMB35 along roots which was perhaps due to differing morphology of
273 the root systems between replicates that gave rise to variable opportunities for root colonization.
274 The lack of meaningful progress of the fluorescent signal in the Bacteria + Protist Treatment
275 between Weeks 2 and 3 may be due, in part, to loss of the fluorescent plasmid, which is usually
276 maintained with 5 μg/mL tetracycline selection. Tetracycline was not added to the μ-rhizoslides

277 to limit interference with plant development, or bacteria may be succumbing to increased predation
278 pressure due to increased numbers of protists.

279 We inoculated roots from the back of the μ-rhizoslides, thus the absence of fluorescent
280 signal in the Bacteria Only Treatment indicates that Rm1021/pCMB35 travelled less than the 5
281 mm distance between the back of the slide and the front when protists were absent. The higher
282 fluorescent signal for the Control Treatment compared with the Bacteria Only Treatment,
283 especially in Weeks 2 and 3, was likely due to root autofluorescence that was more pronounced
284 under this condition.

285 **Quantification of protists and bacteria from plant roots corroborate imaging data and**
286 **indicate protist-assisted transport of inoculated bacteria.** After imaging was complete, μ-
287 rhizoslides were disassembled and the plant roots were divided into upper and lower halves. Roots
288 and the attached soil were transferred to a volume of Page's Saline Solution that was 10x the mass
289 of the root sample and vortexed to disassociate microbial biomass from the roots. Dilutions were
290 spotted on a TY+Tc5 plates and incubated for 3 days to determine bacterial CFUs associate with
291 the root sections. Serial three-fold dilutions were also transferred to a 96-well plate containing
292 Page's Saline Solution and a heat-killed *E. coli* to promote protist growth and reproduction. After
293 one week, the minimum recovered number (MRN) of protists was calculated from the highest
294 dilution that contained reproducing protists.

295 The overall bacterial abundance in the upper sections was equivalent in the Bacteria Only
296 and the Bacteria + Protist treatments despite predation by protists in the latter (Fig 6A). In the
297 lower section of the Bacteria Only treatment strain Rm1021/pCMB35 was not detected, while an
298 average of 1.14×10^5 CFUs of this strain, per 1.0 mg of root tissue, was detected in the lower
299 section of the Bacteria + Protist treatments (Fig 6A). It is important to note that while no

300 fluorescence was detected in the upper half of the Bacteria Only treated roots, Rm1021/pCMB35
301 was still recovered from the roots on which they were inoculated. Additionally, protists were only
302 observed in the Bacteria + Protist Treatment, with comparable numbers in both the upper and
303 lower sections (Fig 6B). More protists may have been present in these sections, as these values are
304 considered the minimum number of recovered protists, true values may be approximately 3x
305 higher because calculation of MRN assumes that the last well of a dilution series contained only
306 one protist at the start of the one-week growth period. These measurements also represent a
307 minimum because they represent bacteria and protists associated with roots; bulk soil which was
308 not evaluated by these methods likely contained additional organisms. Overall, these data indicate
309 that protists not only transported the bacteria along the roots, but that the bacteria were viable after
310 delivery to lower sections of the roots, something that could not be determined by imaging alone.
311
312 **Discussion.** While previous work has shown the potential of using protists as vehicles for
313 transporting particles (19), here we demonstrate their ability to transport beneficial bacteria in a
314 realistic soil system. This transport occurs despite bacterial population loss due to protist grazing.
315 Direct counts of bacteria and protists showed the same order-of-magnitude concentrations
316 of each in the upper sections of the Bacteria Only and the Bacteria + Protists treated μ-rhizoslides.
317 Contrary to this, the imaging experiments showed distinct movement of bacteria only in the
318 Bacteria + Protists treatment. This difference was likely seen because imaging allowed us to
319 discern only populations of bacteria that were growing at high densities, and direct counts allowed
320 us to quantify bacteria not directly assessable to the camera and those that were present in
321 concentrations too low to image. Importantly, *S. meliloti* strain Rm1021/pCMB35 was only
322 recovered from the lower halves of roots treated with Bacteria + Protists, supporting the hypothesis

323 that protists can assist in delivering beneficial bacteria throughout the rhizosphere allowing roots
324 to receive bacterial benefits much quicker and perhaps more uniformly than they would otherwise.
325 Additionally, visualization of bacterial distributions by fluorescent microscopy and image
326 analysis in the Bacteria + Protists treatment showed bacterial proliferation that extended both along
327 the root and horizontally from the root. For the Bacteria Only treatment, distribution was less than
328 5 millimeters from the initial inoculation site in any direction. On their own, bacteria did not spread
329 far enough from the initial inoculation site to reach the front of the μ-rhizoslide where the
330 fluorescence would be visible to the imaging equipment.
331 The protist used in this study, *Colpoda sp*., a ciliate isolated from a legume rhizosphere, is
332 particularly successful in transporting bacteria. Ciliates commonly eat by means of filter feeding,
333 a mechanism of promiscuous consumption of food particles and prey. Bacteria consumed by the
334 ciliates are packaged into a phagosome which is processed and eventually egested from the protist;
335 a process that is not well characterized. It is thought that egested phagosomes break down in the
336 soil and may release viable bacteria which could go on to colonize the area where they were
337 released. How often bacteria can survive intake and egestion, and whether some species are adept
338 at this in not clearly understood. Some bacterial species, for example *Campylobacter jejuni* and
339 *Mycobacterium* spp., are known to escape digestion and colonize the cytoplasm of protists that
340 consumed them (28, 36). Ciliates have also been shown to emerge from feeding on bacterial
341 biofilms with a matrix of bacteria stuck to their cell bodies (19). When the protists travel along
342 plant roots consuming bacteria, both egestion of viable bacteria and physical translocation of
343 bacteria may contribute to protist-assisted transport.
344 The technology described here provides a simple, reproducible experimental system which
345 has the potential to aid in the understanding of rhizosphere dynamics. Of particular interest is

346 bacterial movement in the context of screening a variety of different bacteria/protist/plant/soil
347 combinations for their effects on such movement. For example, protist transportation of
348 *Sinorhizobium sp*. and its effect on nodulation can be studied using this system and parameters that
349 affect transport such as water saturation, soil composition and soil porosity can be readily and
350 tested and quantitated. Protist transport may also be adapted for targeted delivery of other microbes
351 or nano-coated agrochemicals. With increased understanding of such processes, and protist-
352 assisted transport mechanisms, we can begin developing new methods to support sustainable
353 agriculture that is more likely to function in the field.
354
355 **Acknowledgements.** This work was supported by DOE award DE-SC0014522 (to LMS and
356 DJG), NSF award 1605816 (to LMS and DJG), and USDA National Institute of Food and
357 Agriculture award 2016-67013-24412 (to DJG and LMS).
358

References

1. Berendsen RL, Pieterse CMJ, Bakker PAHM. 2012. The rhizosphere microbiome and plant health. Trends Plant Sci 7: 478-486.

2. van Veen JA, Liljeroth E, Lekkerkerk LJA, van de Geijn SC. 1991. Carbon fluxes in plant-soil systems at elevated atmospheric CO_2 levels. Ecol Appl 1:175–181.

3. Guo Y-S, Furrer JM, Kadilak AL, Hinestroza HF, Gage DJ, Cho YK, Shor LM. 2018. Bacterial extracellular polymeric substances amplify water content variability at the pore scale. Front Environ Sci 6:93.

4. Haas D, Défago G. 2005. Biological Control of Soil-borne Pathogens by Fluorescent Pseudomonads. Nat Rev Microbiol 3:307–319.

5. Baveye PC, Otten W, Kravchenko A, Balseiro-Romero M, Beckers É, Chalhoub M, Darnault C, Eickhorst T, Garnier P, Hapca S, Kiranyaz S, Monga O, Mueller CW, Nunan N, Pot V, Schlüter S, Schmidt H, Vogel H-J. 2018. Emergent properties of microbial activity in heterogeneous soil microenvironments: different research approaches are slowly converging, yet major challenges remain. Front Microbiol 9:1929.

6. Jiang X, Zerfaß C, Feng S, Eichmann R, Asally M, Schäfer P, Soyer OS. 2018. Impact of spatial organization on a novel auxotrophic interaction among soil microbes. ISME J 12:1443–1456.

7. Ben-Jacob E, Finkelshtein A, Ariel G, Ingham C. 2016. multispecies swarms of social microorganisms as moving ecosystems. Trends Microbiol 24:257–269.

8. Young IM, Crawford JW. 2004. Interactions and self-organization in the soil-microbe complex. Science 304:1634–7.

9. Cho H, Jönsson H, Campbell K, Melke P, Williams JW, Jedynak B, Stevens AM, Groisman A, Levchenko A. 2007. Self-organization in high-density bacterial colonies: efficient crowd control. PLoS Biol 5:e302.

10. Kim HJ, Boedicker JQ, Choi JW, Ismagilov RF. 2008. defined spatial structure stabilizes a synthetic multispecies bacterial community. Proc Natl Acad Sci 105:18188–18193.

11. Deng J, Orner EP, Chau JF, Anderson EM, Kadilak AL, Rubinstein RL, Bouchillon GM, Goodwin RA, Gage DJ, Shor LM. 2015. Synergistic effects of soil microstructure and bacterial EPS on drying rate in emulated soil micromodels. Soil Biol Biochem 83:116–124.

12. Krome K, Rosenberg K, Bonkowski M, Scheu S. 2009. grazing of protozoa on rhizosphere bacteria alters growth and reproduction of *Arabidopsis thaliana*. Soil Biol Biochem 41:1866–1873.

13. Bonkowski M, Cheng W, Griffiths BS, Alphei J, Scheu S. 2000. microbial-faunal interactions in the rhizosphere and effects on plant growth. Eur J Soil Biol 36:135–147.

394 14. Bonkowski M, Clarholm M. 2012. Stimulation of Plant Growth Through Interactions of
395 bacteria and protozoa: testing the auxiliary microbial loop hypothesis. Acta Protozool.
396 51(3):237-247. DOI: 10.4467/16890027AP.12.019.0765

397 15. Henkes GJ, Kandeler E, Marhan S, Scheu S, Bonkowski M. 2018. Interactions of mycorrhiza
398 and protists in the rhizosphere systemically alter microbial community composition, plant shoot-
399 to-root ratio and within-root system nitrogen allocation. Front Environ Sci 6:117.

400 16. Bouwman LA, Bloem J, van den Boogert PHJF, Bremer F, Hoenderboom GHJ, de Ruiter
401 PC. 1994. short-term and long-term effects of bacterivorous nematodes and nematophagous
402 fungi on carbon and nitrogen mineralization in microcosms. Biol Fertil Soils 17:249–256.

403 17. Bonkowski M. 2004. Protozoa and plant growth: the microbial loop in soil revisited. New
404 Phytol. 162: 617–631

405 18. Rønn R, McCaig AE, Griffiths BS, Prosser JI. 2002. Impact of protozoan grazing on
406 bacterial community structure in soil microcosms. Appl Environ Microbiol 68:6094–105.

407 19. Rubinstein RL, Kadilak AL, Cousens VC, Gage DJ, Shor LM. 2015. Protist-facilitated
408 particle transport using emulated soil micromodels. Environ Sci Technol 49:1384–1391.

409 20. Shor LM, Chau JF, Gage DJ. 2018. Methods and systems to replicate soil properties.

410 21. Gage DJ, Shor LM, Gage JL, Micciulla JL, Rubinstein RL. 2017. Microbial carriers for
411 targeted delivery of agricultural payloads. US9603368B2. US.

412 22. Humphris SN, Bengough AG, Griffiths BS, Kilham K, Rodger S, Stubbs V, Valentine TA,
413 Young IM. 2005. Root cap influences root colonization by *Pseudomonas fluorescens* SBW25 on
414 maize. FEMS Microbiol Ecol 54:123–130.

415 23. Stougaard J. 2000. regulators and regulation of legume root nodule development. Plant
416 Physiol 124:531 LP – 540.

417 24. Lund ZF. 1970. the effect of calcium and its relation to several cations in soybean root
418 growth. Soil Sci Soc Am J 34:456–459.

419 25. Korber DR, Lawrence JR, Sutton B, Caldwell DE. 1989. Effect of laminar flow velocity on
420 the kinetics of surface recolonization by Mot^+ and Mot^- *Pseudomonas fluorescens*. Microb Ecol
421 18:1–19.

422 26. Wang W, Shor LM, LeBoeuf EJ, Wikswo JP, Taghon GL, Kosson DS. 2008. Protozoan
423 migration in bent microfluidic channels. Appl Environ Microbiol 74:1945–9.

424 27. Wang W, Shor LM, LeBoeuf EJ, Wikswo JP, Kosson DS. 2005. Mobility of protozoa
425 through narrow channels. Appl Environ Microbiol 71:4628–4637.

426 28. First MR, Park NY, Berrang ME, Meinersmann RJ, Bernhard JM, Gast RJ, Hollibaugh JT.
427 2012. Ciliate Ingestion and Digestion: flow cytometric measurements and regrowth of a
428 digestion-resistant *Campylobacter jejuni*. J Eukaryot Microbiol 59:12–19.

429 29. Mutalik VK, Guimaraes JC, Cambray G, Lam C, Christoffersen MJ, Mai QA, Tran AB,
430 Paull M, Keasling JD, Arkin AP, Endy D. 2013. Precise and reliable gene expression via
431 standard transcription and translation initiation elements. Nat Methods 10:354–360.

432 30. Silva-Rocha R, Martínez-García E, Calles B, Chavarría M, Arce-Rodríguez A, De Las Heras
433 A, Páez-Espino AD, Durante-Rodríguez G, Kim J, Nikel PI, Platero R, De Lorenzo V. 2013. the
434 standard European vector architecture (SEVA): A coherent platform for the analysis and
435 deployment of complex prokaryotic phenotypes. Nucleic Acids Res 41: D666.

436 31. Le Marié C, Kirchgessner N, Marschall D, Walter A, Hund A. 2014. Rhizoslides: Paper-
437 based growth system for non-destructive, high throughput phenotyping of root development by
438 means of image analysis. Plant Methods 10: 13 (2014). https://doi.org/10.1186/1746-4811 10-13

439 32. Kadilak AL, Rehaag JC, Harrington CA, Shor LM. 2017. A 3D-printed microbial cell culture
440 platform with in situ PEGDA hydrogel barriers for differential substrate delivery.
441 Biomicrofluidics 11:054109.

442 33. Macdonald NP, Zhu F, Hall CJ, Reboud J, Crosier PS, Patton EE, Wlodkowic D, Cooper JM.
443 2016. Assessment of biocompatibility of 3D printed photopolymers using zebrafish embryo
444 toxicity assays. Lab Chip 16:291–7.

445 34. Taerum SJ, Steven B, Gage DJ, Triplett LR. 2020. Validation of a PNA clamping method for
446 reducing host DNA amplification and increasing eukaryotic diversity in rhizosphere microbiome
447 studies. Phytobiomes J 4:291-302. https://doi.org/10.1094/PBIOMES-05-20-0040-TA

448 35. Caspers H. 1978. F. C. Page: An illustrated key to freshwater and soil amoebae with notes on
449 cultivation and ecology. The Ferry House, Far Sawrey, Ambleside, Cumbria: Freshwater
450 Biological Association, Scientific Publication No. 34. 1976. ISSN 0367-1857. 63:289–289.

451 36. Adékambi T, Salah S Ben, Khlif M, Raoult D, Drancourt M. 2006. Survival of environmental
452 mycobacteria in *Acanthamoeba polyphaga*. Appl Environ Microbiol 72:5974–5981.

453 37. Muok, A.R., Claessen, D. & Briegel, A. (2021). Microbial hitchhiking: how *Streptomyces* spores are
454 transported by motile soil bacteria. ISME J: https://doi.org/10.1038/s41396-021-00952-8

455 38. A.R. Muok, A. Briegel. (2021) Intermicrobial Hitchhiking: How Nonmotile Microbes Leverage
456 Communal Motility. Trends in Microbiol 29: 542-550. https://doi.org/10.1016/j.tim.2020.10.005

457 39. William L. King, Terrence H. Bell. (2021). Can dispersal be leveraged to improve microbial inoculant
458 success? Trends in Biotech. https://doi.org/10.1016/j.tibtech.2021.04.008

459 40. Best, AM, Abu Kwaik, Y. Evasion of phagotrophic predation by protist hosts and innate immunity of
460 metazoan hosts by *Legionella pneumophila*. Cellular Microbiol. 2019; 21:e12971.
461 https://doi.org/10.1111/cmi.12971

462

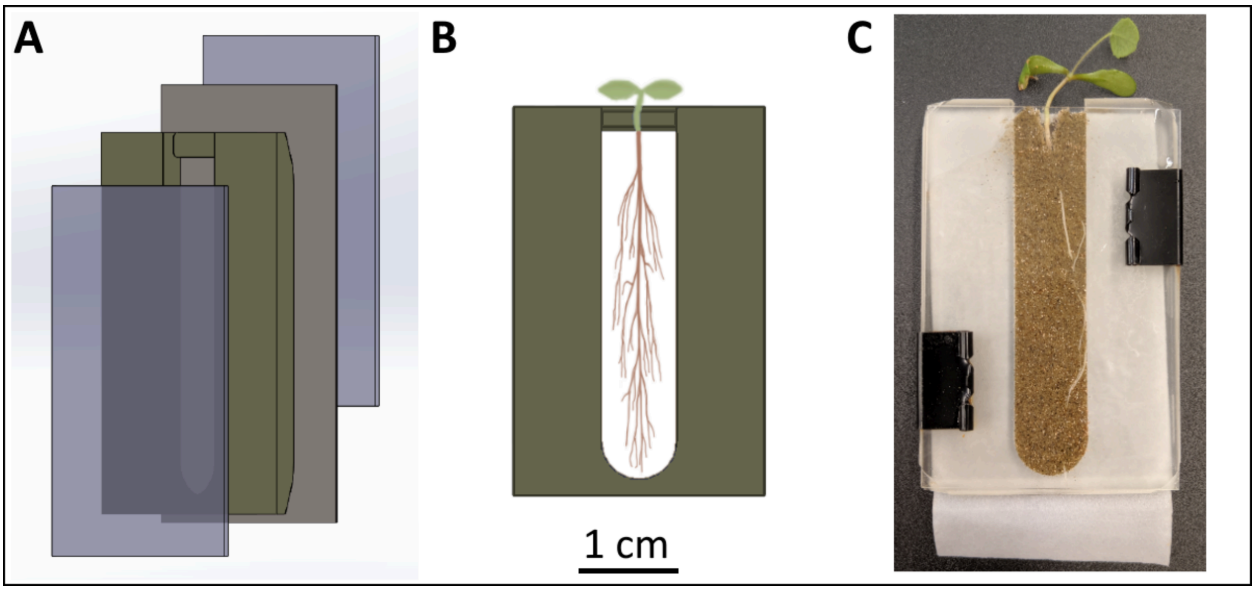

Figure 1. µRhizoslide construction and use. A) CAD drawing of the rhizoslide assembly showing layers including 3D printed rhizoslide spacer and filter paper wick between two glass slides. B) Fully assembled rhizoslide mockup. C) Photograph of rhizoslide in use.

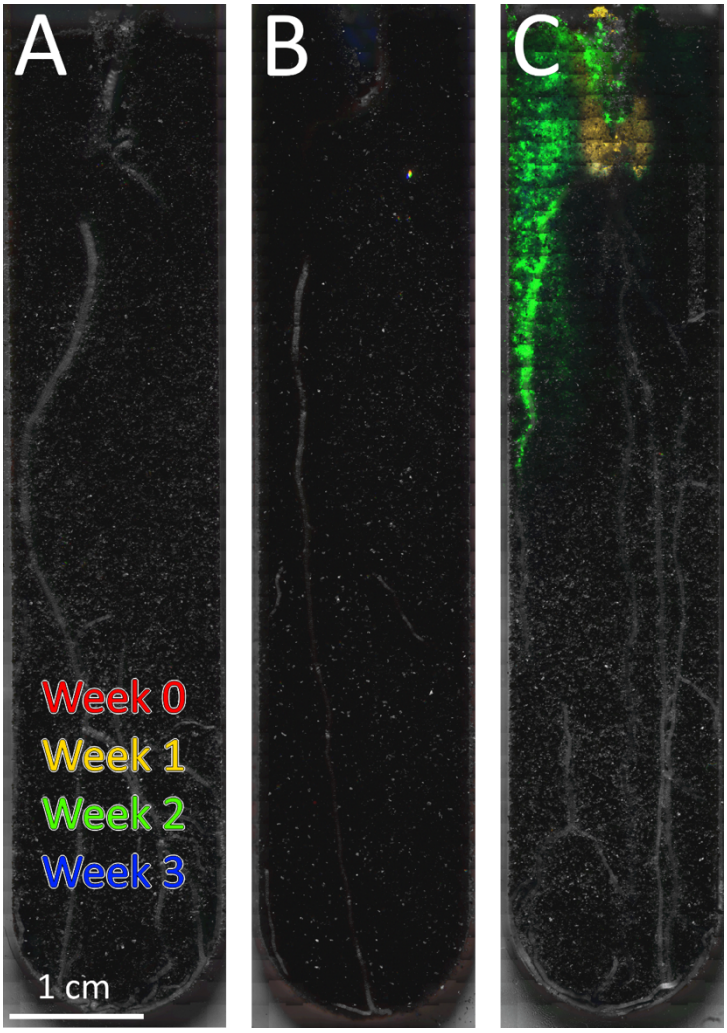

Figure 2 Fluorescent images of plants two weeks post-inoculation. A) Control treatment: inoculated with 10 µL buffer only. B) Bacteria Only treatment: inoculated with 10 µL bacteria suspension. C) Bacteria + Protist treatment: inoculated with 10 µL bacteria suspension with *Colpoda sp.* added.

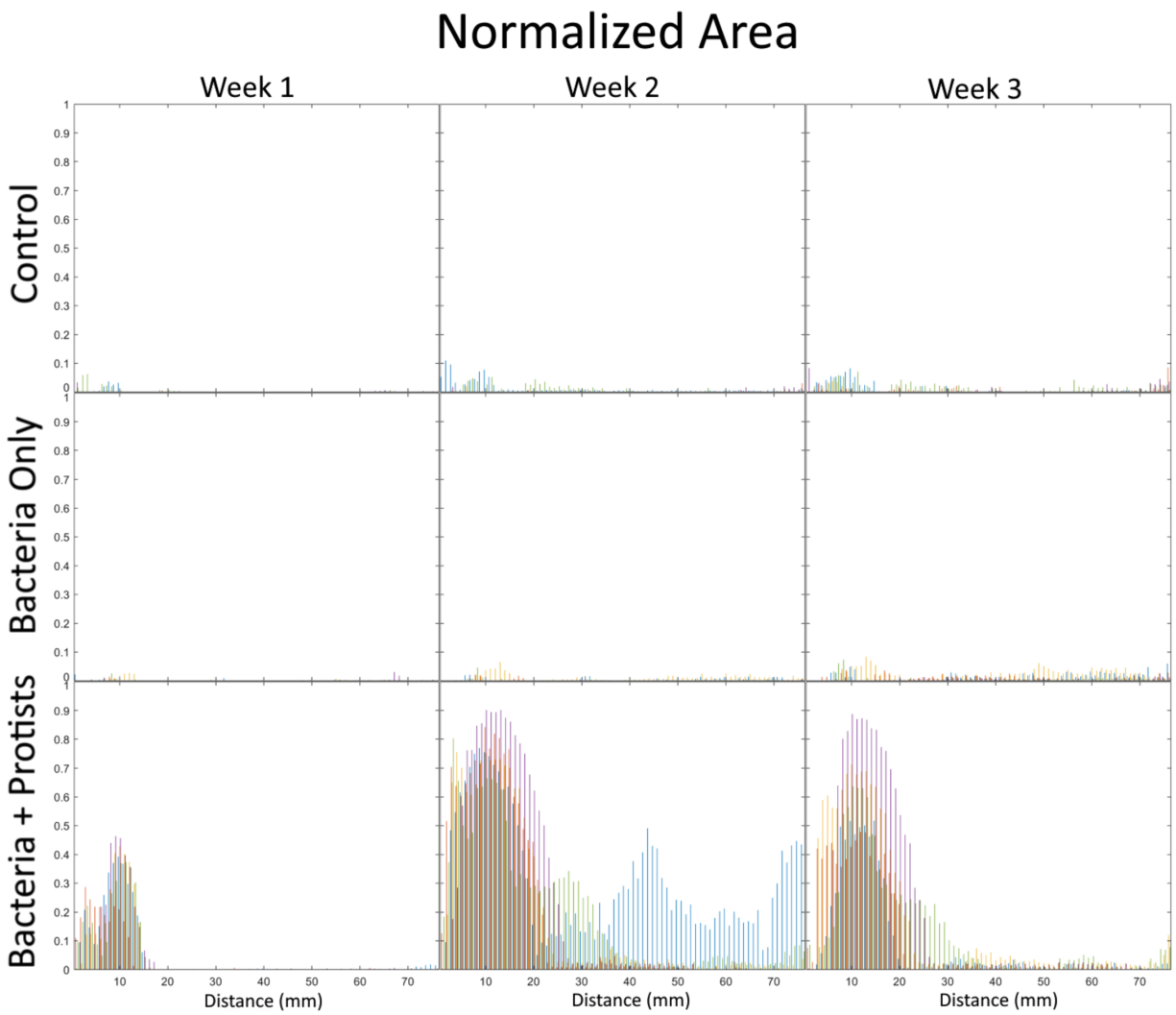

Figure 3 Imaging bacterial movement and growth following plant inoculation with bacteria or bacteria plus protists. For each replicate, the fraction of pixels registering fluorescence in each 1mm image slice is plotted. This normalized fluorescent area is plotted against distance along the root to show the spread of fluorescently labelled bacteria through the rhizosphere. The graphs for each treatment (Control, Bacteria Only, Bacteria + Protists) are plotted in rows, while weeks are shown in columns. Within each graph, replicates are shown by different color bars.

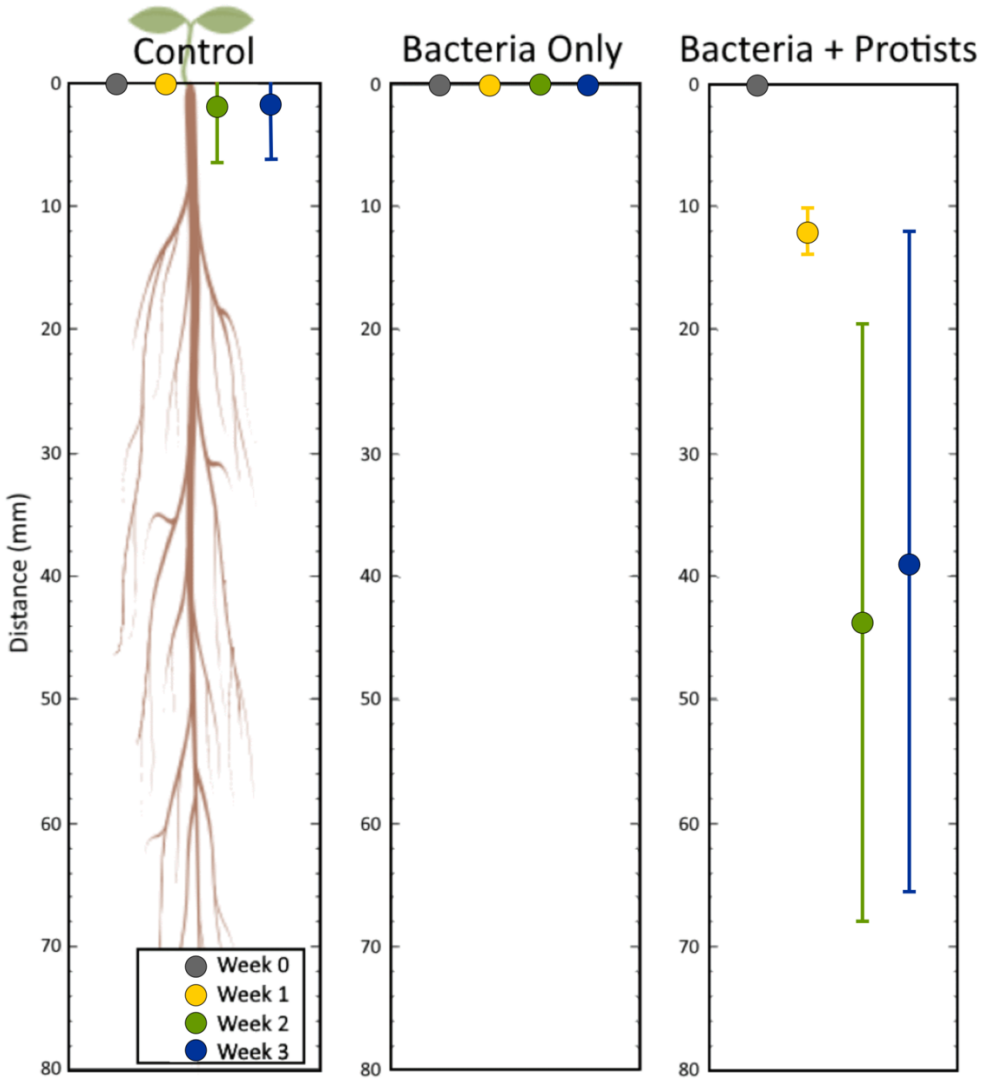

Figure 4 Position of furthest progress of the bacterial fluorescent signal following plant inoculation with bacteria or bacteria plus protists. Marked locations indicate the furthest location along the plant root axis where the fluorescent signal was at least 10% of the total area. A) Control treatment shows no significant shift in position with time ($p > 0.05$). Slight increase in fluorescent signal on some replicates is likely because of root autofluorescence due to nitrogen starvation. B) Bacteria Only treatment shows no shift in position of fluorescent signal with time ($p > 0.05$). C) Bacteria + Protist treatment shows approximately 12 mm of progress in fluorescent signal by Week 1, increasing to 44 mm on average by Week 2. Large deviations between replicates are likely due to root morphology. (n=9, error bars=1 STD).

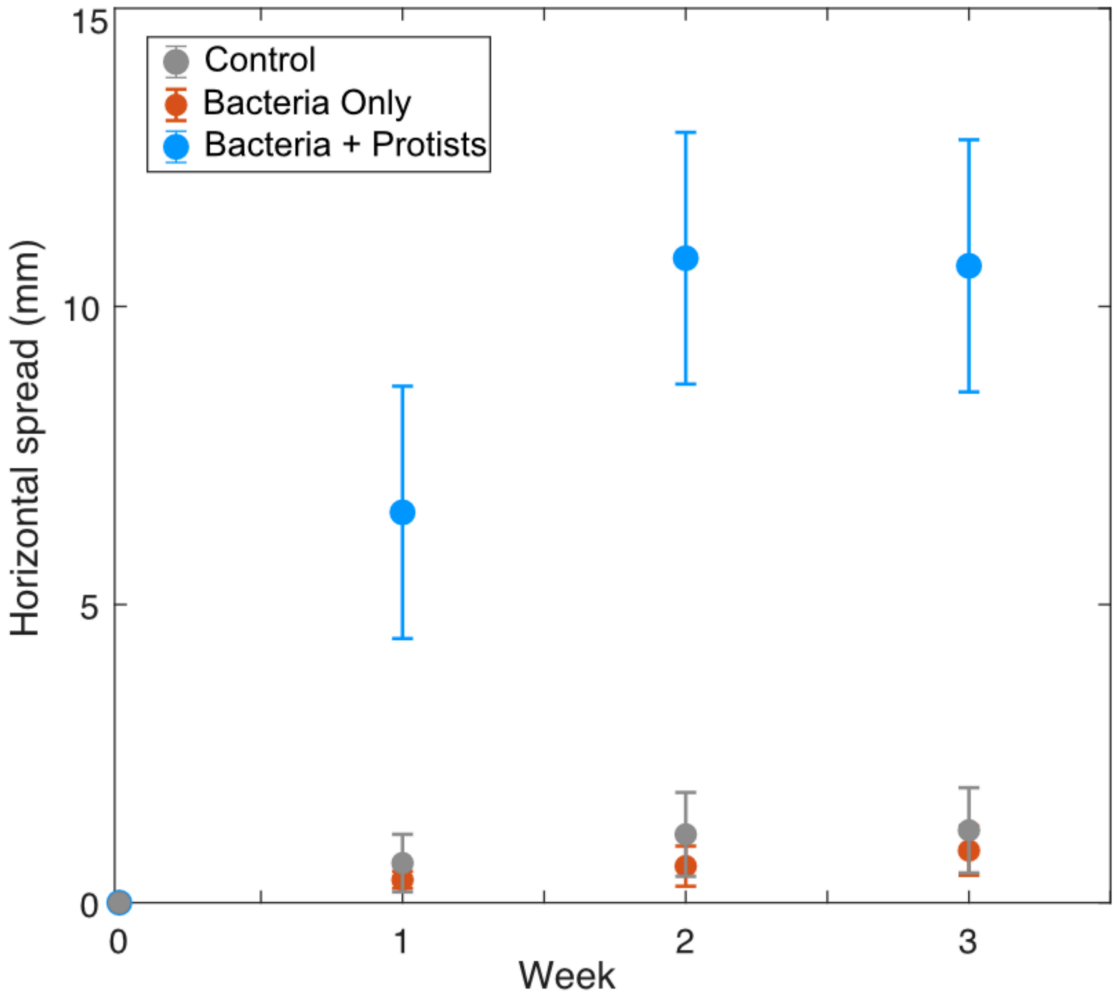

Figure 5 Horizontal spread of the bacterial fluorescent signal following plant inoculation with bacteria or bacteria plus protists. The widest fluorescent area for each replicate was calculated for each week. Marked locations indicate the horizontal width of the fluorescent signal averaged across the replicates. Control and Bacteria Only treatments show widths below 2 mm, which is likely root autofluorescence. Bacteria + Protist treatment shows increasing fluorescence signal width between Weeks 0 and 2, while Weeks 2 and 3 are comparable. (n=9, error bars=1 STD).

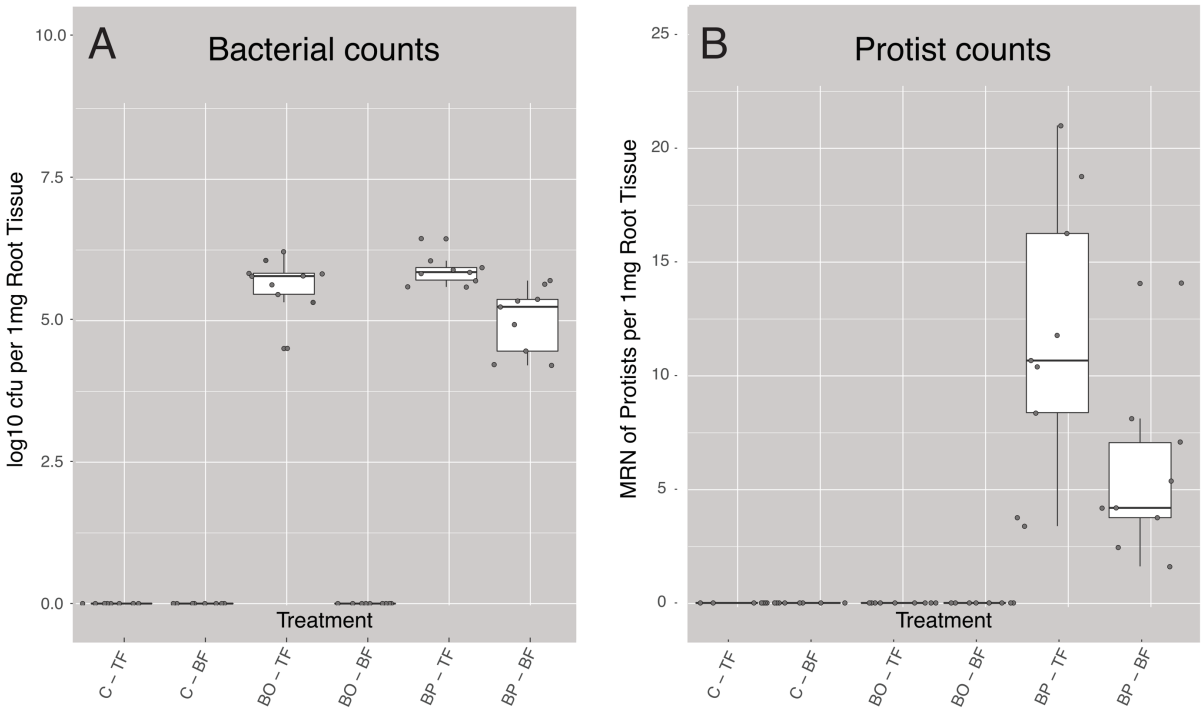

Figure 6 Bacterial and protists counts performed three weeks following plant inoculation with bacteria or bacteria plus protists. The upper and lower sections of *M. truncatula* root systems were separated into top (TF) and bottom (BF) fractions and analyzed for: A) Average bacterial CFUs per 1.0 mg root tissue and B) Average minimum recovered number (MRN) of protists per 1.0 mg root tissue. Control (C) n=8, Bacteria Only (BO) n=9, Bacteria + Protists (BP) n=9